Journal of Geodynamics 152 (2022) 101922

Contents lists available at ScienceDirect

Journal of Geodynamics

journal homepage: www.elsevier.com/locate/jog

Lithosphere structure in the collision zone of the NW Himalayas revealed by alocal earthquake tomography

Irina Medved [a,b,*], Ivan Koulakov [b,c], Sagarika Mukhopadhyay [d], Andrey Jakovlev [b]

[a] *Sobolev Institute of Geology and Mineralogy SB RAS, Prospekt Koptyuga, 3, Novosibirsk 630090, Russia*
[b] *Trofimuk Institute of Petroleum Geology and Geophysics SB RAS, Prospekt Koptyuga, 3, Novosibirsk 630090, Russia*
[c] *Institute of the Earth's Crust SB RAS, Lermontova Street, 128, Irkutsk 664033, Russia*
[d] *Department of Earth Sciences, IIT Roorkee, Roorkee 247667, India*

ARTICLE INFO

Keywords:
Seismic tomography
NW India
Kaurik Chango Rift
Delhi-Haridwar Ridge
NW Himalayas
Collision zone

ABSTRACT

In this study, we obtained new 3D seismic tomography models of the crust and uppermost mantle beneath the northwestern Himalayas down to a depth of 120 km. The data were provided by the India Meteorological Department (IMD) and complemented by the Global International Seismological Centre (ISC) Catalogue. The distribution of anomalies correlates with the main geological features of the region. Specifically, the mountain ranges of the Greater and Lesser Himalaya stand out as a low-velocity anomaly, and the Indian Plate is visible as a high-velocity anomaly underthrusting the Himalayas. The Indian Plate not only underthrusts northwards below the Himalayas, but also bends westwards as it gets closer to the Hindukush Region. A peculiar feature of the model is a high-velocity anomaly in the Kaurik Chango Rift, interpreted as a remnant of the oceanic crust, left after the Indotethys Ocean's closure. In the seismically active Delhi-Haridwar Ridge, a low-velocity upper crustal layer is possibly associated with the sediments of the Indo-Gangetic Plain and with a large number of fault structures. The fragmentation of the Delhi-Haridwar Ridge softens the movement of the Indian Plate to the north, so that the Tethyan Himalaya crust in the area of the Kaurik Chango Fault has remained consolidated and manifests itself as a high-velocity anomaly.

Data Availability: The full directory of LOTOS code with data corresponding to this study is available at https://doi.org/10.5281/zenodo.5519210 (accessed on 23 September 2021).

1. Introduction

The Indo-Asian collision is the main cause of tectonic processes in Asia. They comprise the movement of strong lithospheric blocks, such as the Tarim and Junggar, the emergence of mountain structures, ranging from the Himalayas and Tibet to the Sayan Mountains (Buslov et al., 2004). The entire system is set in motion by the Indian indenter, which moves northwards at a speed of ~50 mm/year. Moreover, about 50 % of the total shortening is accommodated within the Himalayas (England and Molnar, 1997; Larson et al., 1999; Banerjee, Bürgmann, 2002). The Himalayan mountain system stretches for 2500 km from the west to east and is divided into the western (Jammu and Kashmir, Himachal Pradesh, Uttarakhand), central (Nepal, Sikkim), and eastern (Bhutan, Arunachal Pradesh) segments (Thakur, 1992; Yin, 2006; Gupta and Gahalaut et al., 2014). The study region belongs to the northwestern Himalayas and includes the regions of Uttarakhand, Himachal Pradesh, and part of Jammu and Kashmir.

The two main global geological structures in the region under consideration are the Indian Plate and the Himalayas, which are subdivided into smaller discrete structures. The Himalayas in the study area are subdivided into the Siwalik Himalaya (Tertiary strata), Lesser Himalaya (non-fossiliferous low-grade metamorphic rocks), Greater Himalaya (crystalline complex composed of gneisses and aplitic granites), and Tethyan Himalaya (marine, fossiliferous strata) (Gupta and Gahalaut, 2014). Fig. 1 depicts the major structural geological features of the Himalayas in the study region: the Main Frontal Thrust (MFT) situated between the sediments of the Indo-Gangetic Plain and Siwalik Himalaya, Main Boundary Thrust (MBT) south of the Lesser Himalaya, Main Central Thrust (MCT) between the Lesser and Greater Himalaya, and the South Tibet Detachment (STD) between the Greater and Tethyan Himalaya. The northern boundary of the Tethyan Himalaya is represented by the Indus-Tsangpo Suture Zone (ITSZ) (Chatterjee et al., 2013;

* Corresponding author at: Sobolev Institute of Geology and Mineralogy SB RAS, Prospekt Koptyuga, 3, Novosibirsk 630090, Russia.
E-mail address: Zabelirina@yandex.ru (I. Medved).

https://doi.org/10.1016/j.jog.2022.101922
Received 24 January 2022; Received in revised form 10 May 2022; Accepted 29 May 2022
Available online 1 June 2022

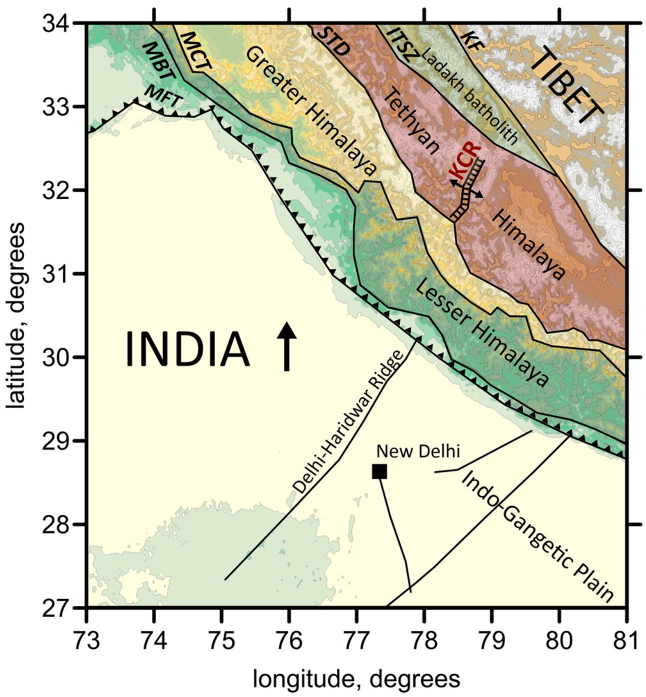

Fig. 1. Map of the main tectonic units in the study region (Guillot et al., 2003). Geological units are highlighted by different colors. Lines mark the major faults of the region from Gansser (1964). Faults: ITSZ – the Indus-Tsangpo Suture Zone; MBT – the Main Boundary Thrust; MCT – the Main Central Thrust; MFT – the Main Frontal Thrust; STD – the South Tibet Detachment; KCR – the Kaurik Chango Rift.

Gupta and Gahalaut, 2014).

The largest thrust earthquakes in the Himalaya take place on the seismogenic detachment under the Siwalik and Lesser Himalaya, whereas the small and moderate earthquakes of the Himalayan seismic belt originate in the downdip part of the seismogenic detachment or on the mid-crustal ramp (Gupta and Gahalaut, 2014).

In the considered region, the Kaurik Chango Rift is an area of particular interest. It is one of the north-south trending active rift zones in the Trans-Himalaya Tibetan Plateau, which extend from the Tibetan Plateau to the Greater Himalaya (Armijo et al., 1986; Gupta et al., 2014; Ni and Barazangi, 1985; Arora et al., 2012). The Kaurik Chango Rift is one of the most active rift zones and goes deep into the Himalayan Arc. A slip rate of the 100-km-long Kaurik Chango Rift is ~1 cm/year, with seismic activity occurring up to a25 km depth. The slip on the north-south normal fault of the Kaurik Chango Rift brings about stress reduction to the south in the active detachment zone beneath the Outer and Lesser Himalaya (Arora et al., 2012). It bears mentioning that the Kaurik Chango Rift is located on the northern continuation of the Delhi-Haridwar Ridge – one of the subsurface ridges below the Indo-Gangetic Plain. There are three such ridges from the east to west: the Munger-Saharsa Ridge, the Faizabad Ridge and the Delhi-Haridwar Ridge (Gahalaut and Kundu, 2012). These ridges are believed to be high topographic features seated on the Indian Shield or on the basement rocks. Despite their existence, the Indo-Gangetic Plain is very smooth consequent to the occurrence of sediments whose thickness reaches 6–7 km (Miglani et al., 2014). Possibly, there is a continuation of the Delhi-Haridwar Ridge under the Himalayan Arc (Arora et al., 1982; Lilley et al., 1981). Chandra (1978) pointed out that the activity along the Kaurik Chango Rift may be impacted by the subducting Delhi-Haridwar Ridge. Furthermore, the subsurface ridges delineate the ruptures of the great Himalayan earthquakes (Gahalaut and Kundu, 2012).

Geophysical surveys: The Indo-Asian collision zone is highly popular among the researchers. There are huge number of regional seismic tomography models, for example (Maurya et al., 2016; Acton et al., 2010; Replumaz et al., 2004), showing a subsidence of the Indian Plate under the Himalayas. The individual Himalayan regions are typified by a large number of local deep-structure models based, for instance, on the methods of local earthquake tomography (Koulakov et al., 2015;Raoof et al., 2017; Diehl et al., 2017; Mukhopadhyay and Sharma, 2010), attenuation tomography (Thirunavukarasu et al., 2016; Guo et al., 2012; Sheehan et al., 2014), receiver functions (Rai et al., 2006; Oreshin et al., 2011; Mitra et al., 2005; Kumar et al., 2005; Singh and Kumar, 2009). However, the western region seems to be neglected. There are only a few local models for the region, for example (Kumar et al., 2019; Bhatti et al., 2018), which mainly exhibit the region's general structure. In this regard, according to (Bhatti et al., 2018; Kumar et al., 2019), the crust under the Himalayas stands out as low-velocity anomalies, its thickness increasing from the south to north. The Indian Plate gradually sinks to the north up to the Karakoram Fault, and then the dip angle sharply increases (Bhatti et al., 2018). As known, the Kohistan-Ladakh Arc is sandwiched between the Indian and Asian plates. Additionally, the Neo-Tethyan oceanic crust immerses beneath the Eurasian Plate in the Ladakh Arc.

The region around the city of New Delhi is characterized by an increased seismicity rate posing a danger to the local population (Bansal et al., 2021). Subsequent to Gupta et al. (2013), the tomographic models are consistent with the tectonic features in the region. According to Kumar et al. (2017), the Indo-Gangetic Plain manifests itself as low-velocity anomalies.

The bulk of research on the northwestern Himalayas is based on the receiver function method, for instance (Xu et al., 2021, 2018; Oreshin et. al, 2011, Rai et al., 2006). The average crustal thickness on the Indian Plate has been found to be ~35 km. The Moho boundary lies at a depth of ~40 km under the Indo-Gangetic Plain and MFT, ~50–55 km under the MBT, and up to 60 km under the Himalayas. Further, from the Karakoram Fault to the north, the Moho boundary goes to depth, reaching 80 km under Tibet. According to Oreshin et al. (2011), the high S-wave velocities in the MBT indicate that the adjacent region almost entirely consists of mafic rock.

In the presented investigation, we have created new seismic models of the crust and uppermost mantle to a depth of 120 km, which reveal the structure of the NW Himalaya and Delhi-Haridwar Ridge. In addition, the results obtained will help to clarify the relationship between the Kaurik Chango Rift and Delhi-Haridwar Ridge: this aspect has not been evident from the results of previous seismological studies.

2. Data and method

The arrival time data for the research were provided by the India Meteorological Department (IMD, 2021) and complemented by the International Seismological Centre (2021) within the limits 26–35°N and 69–100°E. Both catalogs included the arrival times of the P and S waves from regional seismicity recorded by stations in the time period 1950–2016. The IMD provided the data with permanent stations, whereas the data from the ISC catalogue included both permanent and temporary stations. When merging the IMD and ISC catalogues, we identified the common events with close origin times (<2 s) and coordinates (<50 km). After combining the arrival times from both databases, the sources were relocated using the location algorithms in the LOTOS code.

In total, after merging the datasets, we obtained 23,769 earthquakes recorded by about 80 stations. The number of picks was 226,362, including 134,968 P-rays and 91,394 S-rays. Note that we are not working with seismograms. The phases of the IMD catalog were manually picked by other scientists.

The research was carried out with the LOTOS seismic tomography algorithm. It is based on an iterative calculation of 3D models for P- and S-velocities, and on event location. There are three general steps of

LOTOS algorithm: 1. Preliminary location of sources; 2. Location of sources in the 3D velocity model; 3. Simultaneous inversion for the source parameters and velocity model using several parameterization grids. Steps 2 and 3 are repeated in turn one after another in several iterations. There were 5 iterations in our case. 3D models of P and S wave velocities are obtained at the output.

Before starting the inversion, a part of the data was rejected according to two criteria. The first one is related to the number of picks recorded from an earthquake at the network stations. In our case, earthquakes with less than 8 picks were not used in the inversion. The second criterion: the residuals should not exceed 1 s. They were obtained during the event location stage in the starting 1D model. After filtering the data, there were 3699 events left, the number of picks being 44,457 with the corresponding 25,461 P-wave rays and 18,996 S-wave rays. Thus, on average, 12 picks were used per event, but not less than 8 picks. Fig. 2 illustrates the source and receiver locations as well as the ray coverage for the horizontal and vertical sections.

As a reference model, we used the 1D P- and S- velocity distributions set at some depths and linearly interpolated. Velocity perturbations in this model were estimated iteratively in relation to the initial velocity model. In the first iteration, we defined the velocities corresponding to the areas of the regional Tien Shan collision, which were previously studied in Sychev et al. (2018). After completing a full cycle of the tomographic inversion, we computed average velocities at individual depths and used them to set a 1D reference model for the next cycle of calculations. After several such iterations, the amount of positive and negative anomalies in the resulting model turned out to be balanced. This fact indicated the adequacy of the reference model employed. The parameters of the 1D reference model involved for computing the main results are given in Fig. 3.

Variance reduction and residuals after each iteration are presented in Table 1. Histograms of P-wave traveltime residuals before and after the inversion are shown in Fig. 4.

The LOTOS algorithm has existed for over 15 years and been an instrument to build a large number of seismic models for various regions around the world, including collision zones, for example, Nepal (Koulakov et al., 2015), Indo-Asian collision (Koulakov et al., 2018), Caucasus (Zabelina et al., 2016), Turkey (Medved et al., 2021), Tien Shan

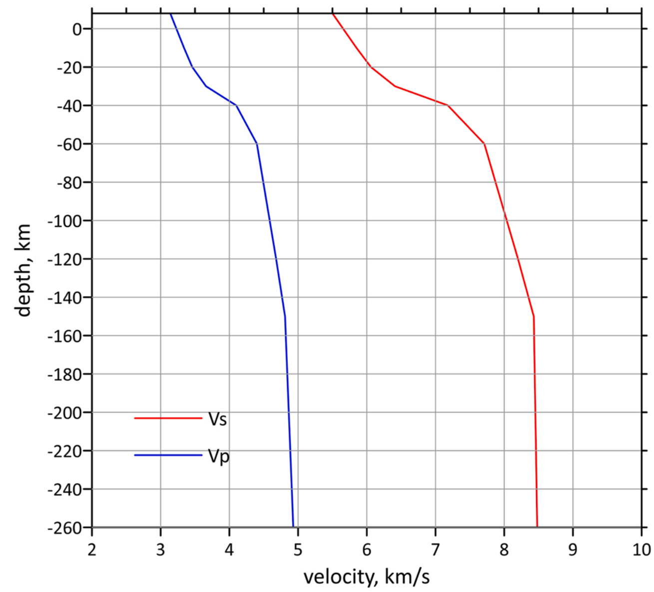

Fig. 3. 1D reference model. Red line indicates P-velocity, blue line indicates S-velocity.

Table 1
Values of the P and S wave residuals and their reduction during the iterative tomographic data inversion. AMR stands for absolute mean residuals in L1 norm.

Iteration	AMR of dtP, s	Variance Reduction, dtP, %	AMR of dtS, s	Variance Reduction, dtS, %
1	0.680	0.00	1.050	0.00
2	0.585	13.8	0.838	20.2
3	0.575	15.3	0.787	25. 0
4	0.567	16.5	0.771	26.5
5	0.564	17.0	0.757	27.9

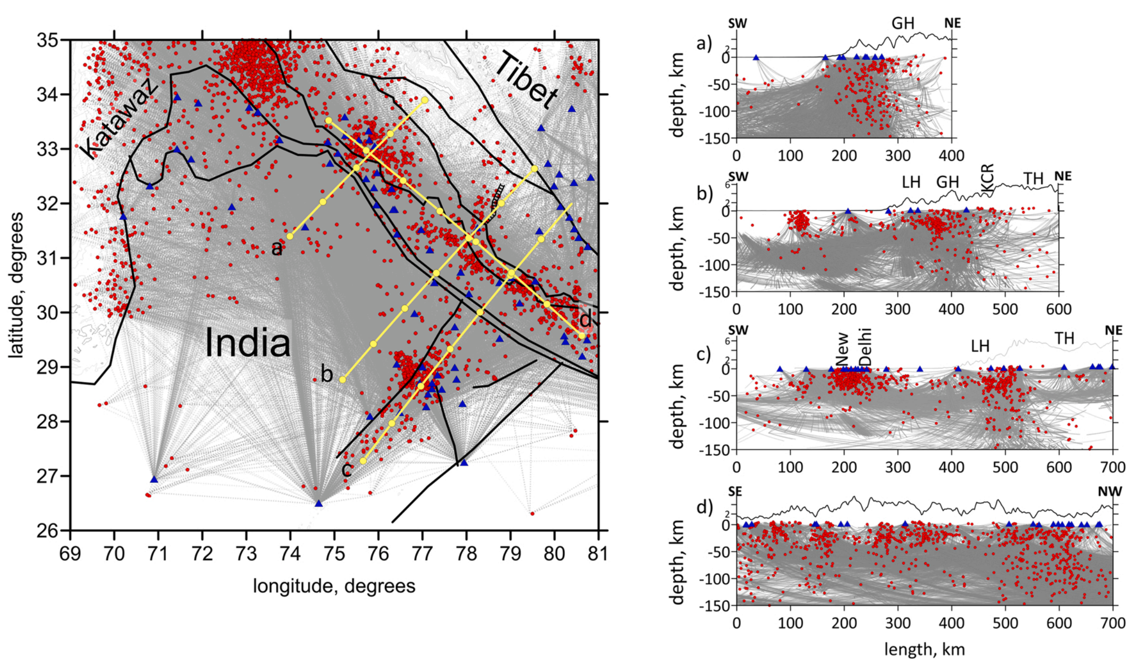

Fig. 2. Ray coverage of the initial region. Red dots are the earthquakes; blue triangles are the stations; lines are the main faults. Yellow lines are locations of the profiles; Black lines at the top of the profiles show topography. Abbreviations: KCR – the Kaurik Chango Rift, LH – the Lesser Himalaya, GH – the Greater Himalaya, TH – the Tethyan Himalaya.

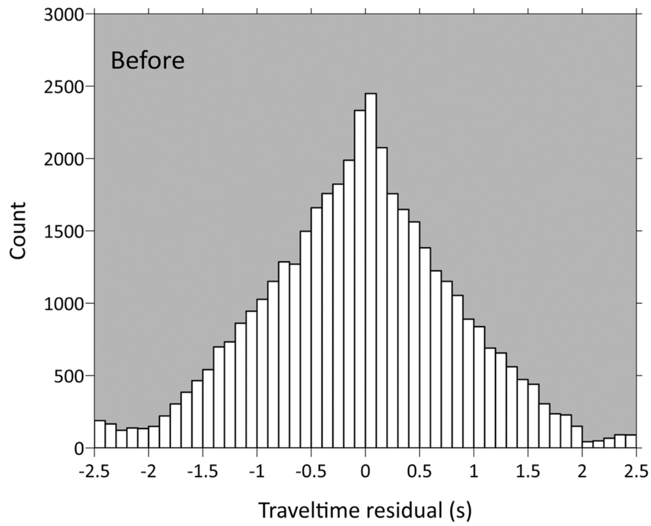

Fig. 4. Histograms of P-wave traveltime residuals before (left) and after (right) inversion.

(Medved et al., 2021) and others. Details on the features of the method are given in the article (Koulakov, 2009). In addition, one can perform inversion with the data used in this study and obtain the same results as presented here by running the code, which is available at the Zenodo link: https://doi.org/10.5281/zenodo.5519210.

3. Seismic tomography results and testing

The results of this work are presented in the form of horizontal and vertical velocity models in Figs. 5 and 6 respectively. The horizontal sections of the P- and S-wave velocity anomalies models are shown at 20, 40, 60 and 80 km depths together with the main fault structures of the region as well as the Kaurik Chango Rift and Delhi-Haridwar Ridge. Fig. 6 (III) gives four vertical sections of the interest with P- and S-wave

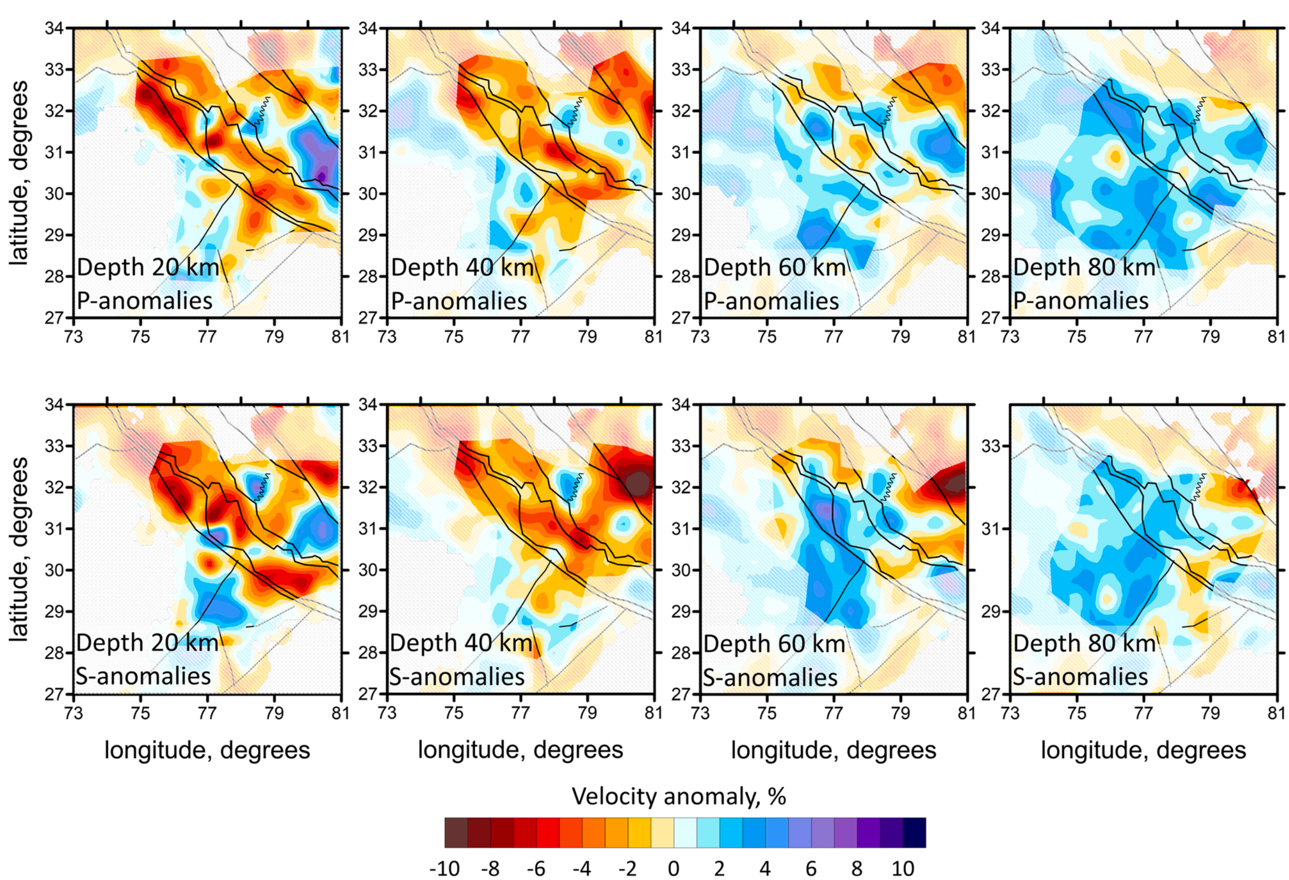

Fig. 5. Horizontal sections of the seismic tomography models at 20, 40, 60 and 80 km depths. The anomalies are plotted with respect to the reference model shown in Fig. 3. At the top are P-anomalies; at the bottom are S-anomalies. Black lines mark the major faults of the region from Gansser (1964), and curved line is the Kaurik Chango Rift. Blank regions depict areas with a low resolution.

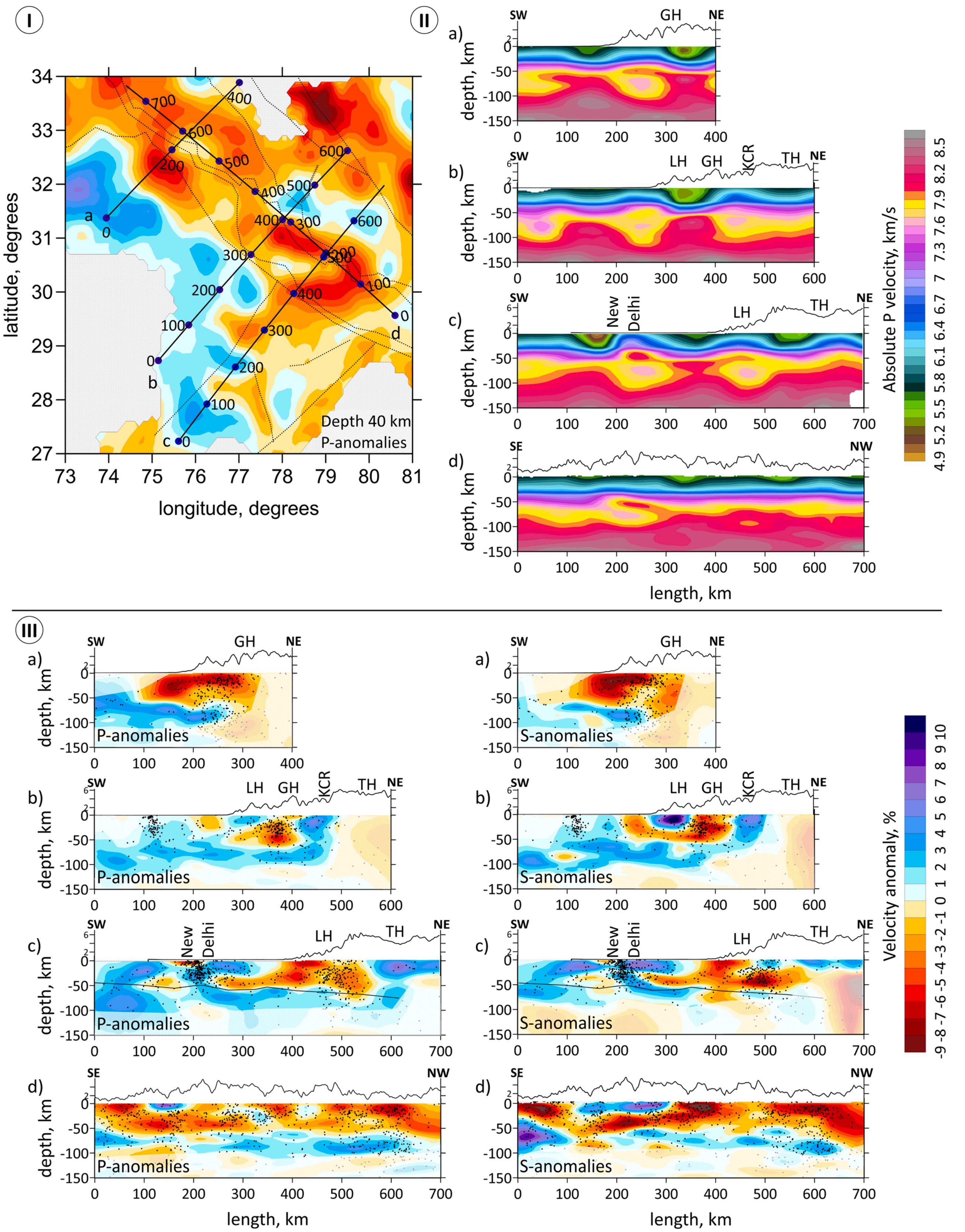

Fig. 6. Vertical sections of the seismic tomography models and absolute velocitites. I) Locations of vertical sections; II) Absolute velocities on vertical sections; III) Seismic tomography results on the vertical sections: P-anomalies on the left, S-anomalies on the right. The line on c profile is the Moho depth from (Priestley et al., 2008). Black lines at the top of profiles are topography. Black dots are earthquakes' hypocentres. Abbreviations: KCR – the Kaurik Chango Rift, LH – the Lesser Himalaya, GH – the Greater Himalaya, TH – the Tethyan Himalaya.

velocity anomalies. The first three sections are defined across the strike of the Himalayan Arc: the first one (a) runs in the northwestern part, second (b) passes through the Kaurik Chango Rift, and third (c) extends along the Delhi-Haridwar Ridge. The fourth profile (d) runs along the Himalayas perpendicularly to the first three profiles.

3.1. Model validation

The velocity structure of the lithosphere in the study area correlates well with the major geological units: the Indian Plate is evident as high-velocity anomalies, with the Himalayas being characterized by low-velocity ones. The main faults are also associated with low velocities. This is one of the important criteria for assessing the reliability of the results. Another criterion is the similarity of models for P- and S-anomalies. As can be seen in Fig. 5, the models in the present case are similar, except for the small artifact anomalies. The main cause of the differences is the lesser number of picks for S waves and low ray coverage density. The reliability of future results can be judged by the location of the observation network. For instance, according to Fig. 2, the western part of the exploration area near Katawaz and Tibet have a low ray density and a small number of the stations. Thus, the anomalies obtained in these regions are considered not reliable.

In addition to the above criteria, there are a number of synthetic tests to check the resolution. In this study, we carried out the checkerboard simulation for the horizontal and vertical sections in Figs. 7 and 8 respectively, and a synthetic test with realistic anomalies in Fig. 9. The size of the anomaly for the horizontal sections of the checkerboard was chosen to be 80 × 80 km. Following the test, the checkerboard patterns were not reproduced even at a depth of 20 km in the regions of Katawaz, Ladakh and Tibet with a low ray density. In contrast, the resolution is good within the latitude range 28°N - 33°N and longitude range 76°E - 81°E. For this reason, we decided to choose the smaller study region for discussion. Moreover, as follows from the horizontal sections in the checkerboard test (Fig. 7), at depths exceeding 80 km the anomalies are smeared in the northwestern direction, which is due to the dominant ray distribution. This feature should be taken into account during the interpretation.

The vertical resolution was tested through the checkerboard test for the vertical sections presented in Fig. 8. The test results show that anomalies with size of at least 100 × 80 km are reliably restored to a depth of ~120 km. According to the results from the b and c sections, the anomalies under the Delhi Haridwar Ridge, Lesser Himalaya and Greater Himalaya area are well resolved up to 120 km depth. This can be explained by a large number of events, which can be seen in Fig. 2.

In the horizontal sections of the checkerboard test, the resolution of the NW area of the study region is poor. The test in Fig. 8(III) demonstrates a smeared structure at the NE side of the section a under the Greater Himalaya, as well as at the NW side of the section d. The configuration of the checkerboard structure under the Tethyan Himalaya and the Kaurik Chango rift region remains poorly resolved.

In order to clearly estimate the resolution in the Kaurik Chango Rift area and Tethyan Himalaya, the test with realistic anomalies for the section b was done, which is presented in Fig. 9. The size of the KCR high-velocity anomaly was set 100 km laterally and 50 km in thickness, with an amplitude of 4 %. The sizes of near-surface anomalies under the LH and GH regions were set 80 km by size. The lateral size of the deep great high-velocity anomaly was set 200 km. All the amplitudes are given in Fig. 9 (column 1). According to the reconstructed models, the low-velocity anomaly under TH is smeared, but anomalies under the Delhi Haridwar Ridge, LH and GH are reconstructed. Therefore, this test demonstrated the robustness of velocity structures beneath the rift zone having a characteristic size of ~ 100 × 100 km.

The synthetic testing exhibits a problem of poor determination of depths for the most of sources due to the uneven distribution of seismic stations in our dataset. After the iterative inversion, the events appeared strongly biased in the vertical direction. This demonstrates that we should be prudent about the derived depth distribution of seismicity after inversion of the experimental data shown in Fig. 2. At the same time, we see that despite strong mislocations of the events, the main velocity structures in our synthetic models are restored correctly. Thus, an important conclusion following from this series of synthetic tests is that we can trust the distribution of velocity anomalies, but should be careful when interpreting the locations of the events.

4. Interpretation

The main features of the region are a low-velocity anomaly under the Lesser and Greater Himalayas located within the Himalayan Arc between the MFT and STD, and a high-velocity anomaly in the Indian Plate region. These features have been observed in many existing seismic tomography models (e.g., Bijwaard et al. (1998), Koulakov et al. (2015), Maurya et al. (2016), Replumaz et al. (2004)]. The low velocities within the Himalayan Arc are associated with the accretionary Himalayan mountain range that is mechanically softer compared to the consolidated Indian Plate. Although the seismic tomography employed in this research does not technically allow delineating the Moho boundary, the vertical sections in Fig. 6 suggest that the low-velocity anomaly related to the Himalayan Arc reaches a depth of ~50–60 km. This corresponds to the generally accepted Moho depth in the region (Xu et al., 2021; Priestley et al., 2008, 2019; Subedi et al., 2018; Oreshin et al., 2011). We plotted the Moho boundary from Priestley et al. (2008) on the vertical section c, which clearly outlined the low-velocity anomaly confined to the Himalayan Arc (Fig. 6). In the section d the boundary of the Himalayan low-velocity anomaly, which appears to be the Moho boundary, is deeper under the northwestern Himalayas in the study region than below their southeastern part. This indicates that the Indian Plate is bending down towards the northwest as it approaches the Pamir-Hindukush Region. The thickness of the low-velocity crust also seems to vary along the strike of the Himalayas as is observed from the section d. Similar variation was observed for the Nepal Himalayas by Koulakov et al. (2015) and the Eastern Himalayas by Raoof et al. (2017).

The consolidated Indian Plate, like a monolith, stands out as a high-velocity anomaly. In the vertical a, b, c sections (Fig. 6), one can evidence the trend of the anomaly subsiding under the Himalayas. It is noted that the pattern and trend of the high-velocity anomaly along these three sections differ from each other in many respects. Interestingly, the dip angle of the anomaly in the northwestern part of the study area (section a) is steeper than in the southeastern part. This feature can also be observed in the section d. Regarding the section a, the Indian anomaly plunges underneath the Himalayas near the MFT, whereas in b and c the subsidence begins much earlier in relation to the major Himalayan faults, and it is virtually sub-horizontal in section b. The observed feature is hidden below the large sedimentary cover of the Indo-Gangetic Basin, which is about 6–7 km, as it follows from Miglani et al. (2014).

In the horizontal 20 km section at a depth of 20 km (Fig. 5), linear low-velocity anomalies are distinguished in the Delhi-Haridwar Ridge area. These structures are consistent with the locations of the main faults abundant in the region under consideration (Sandhu et al., 2018). The vertical section c in Fig. 6 (III) demonstrates a heterogeneity of the velocity structure below the Indo-Gangetic Plain to a depth of 50 km. The observed structural features on the surface and in the crust are likely to result from the weakening of the crust due to a large number of faults, which is confirmed by the results of gravimetry (Ravi Kumar et al., 2013). Compared to the rest of the Indian Plate, the heavily fragmented Delhi-Haridwar Ridge most probably should exhibit more plastic properties.

Some researchers have suggested a link between the Delhi-Haridwar Ridge and Kaurik Chango Rift. For example, (Arora et al., 1982; Lilley et al., 1981) admit that the Delhi-Haridwar Ridge may be underthrusting the Himalayas, causing seismic activity in the Kaurik Chango Rift (Chandra et al., 1978). Along the section c we also observe a new front

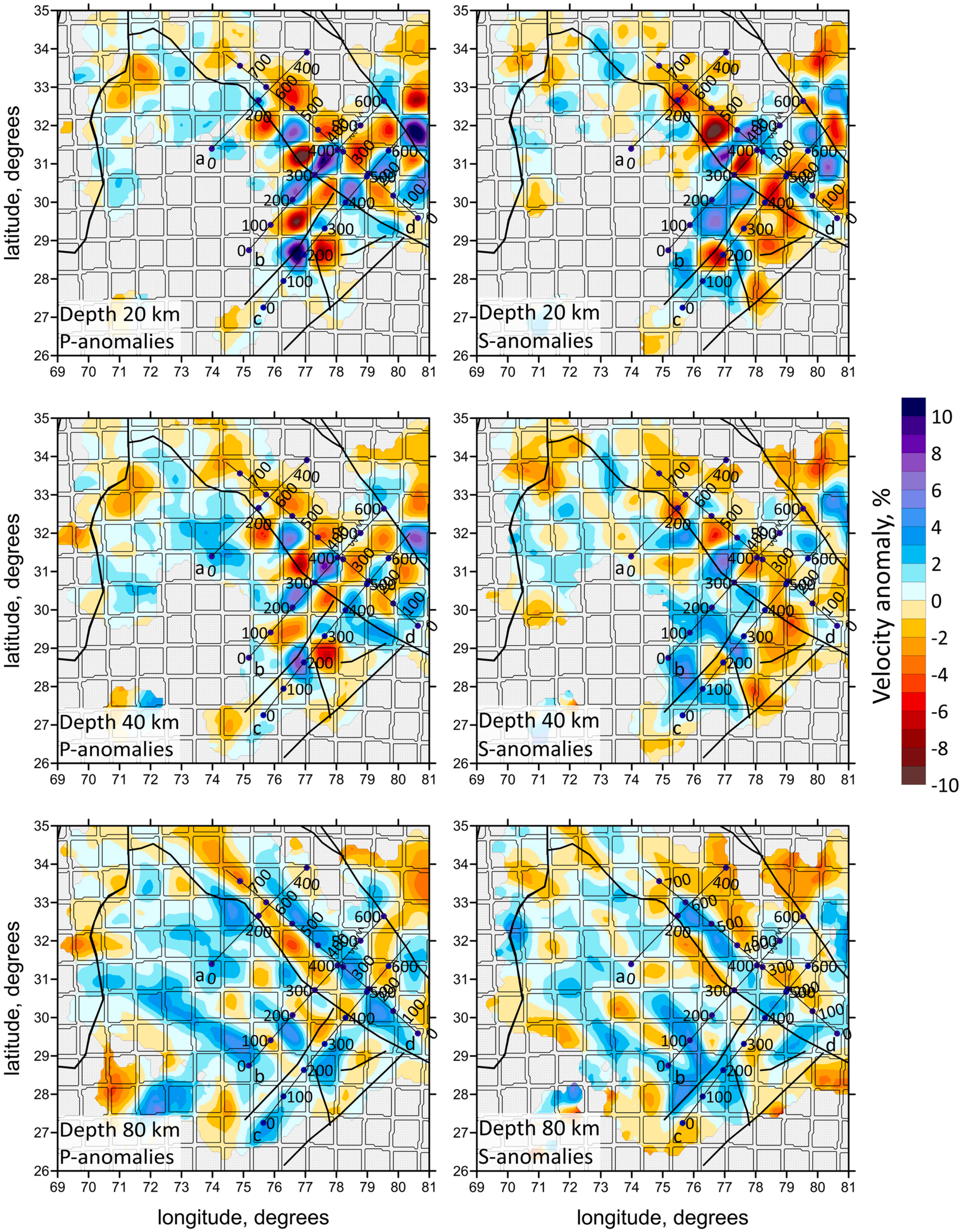

Fig. 7. Horizontal models in the checkerboard test at 20, 40 and 80 km depths, the size of anomaly is 80 km.

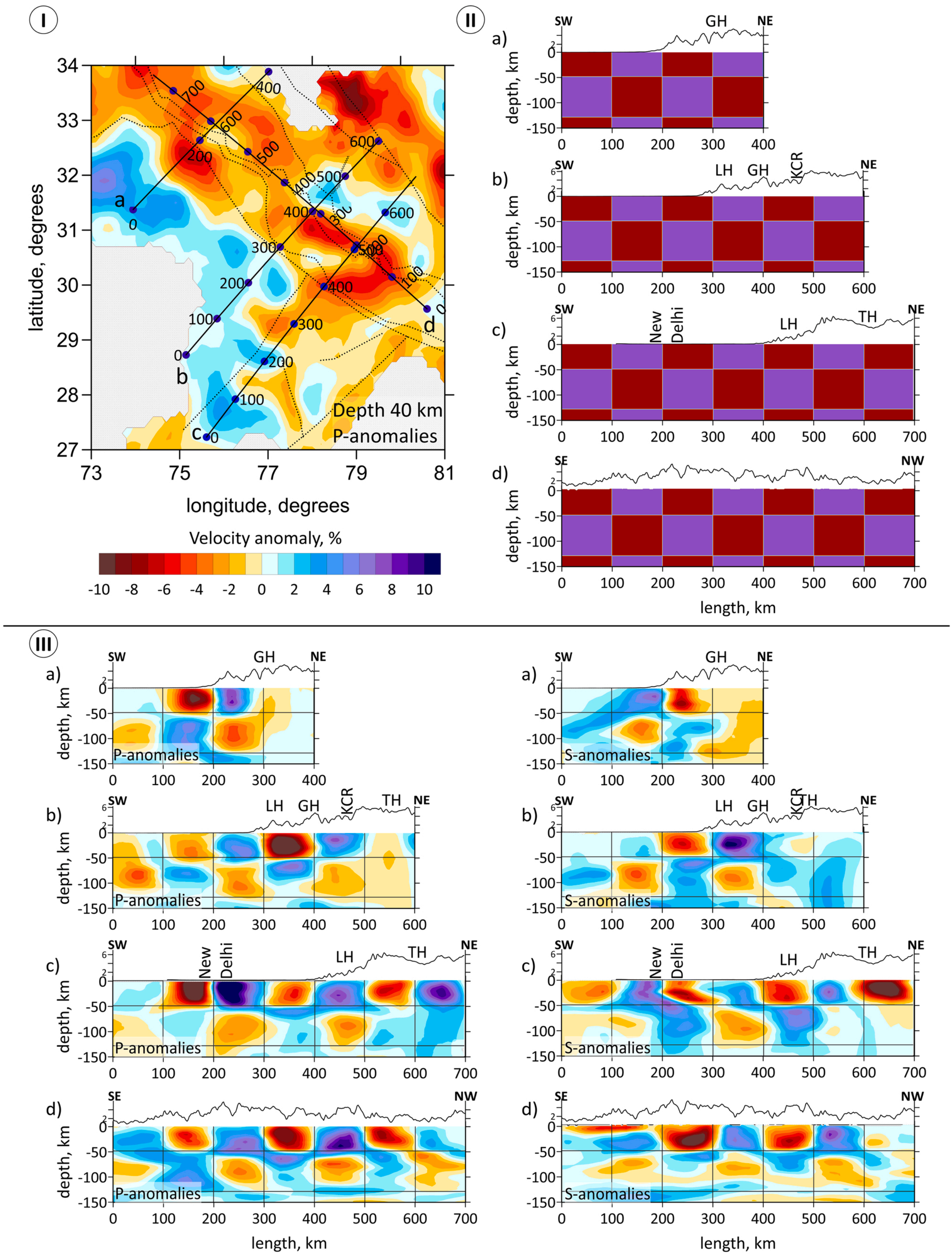

Fig. 8. Vertical sections on the checkerboard test. I) Horizontal section at 40 km depth with locations of vertical sections; II) Input checkerboard models for vertical sections; III) Vertical models of checkerboard test for P (at the left) and S (at the right) velocity anomaly. Abbreviations: KCR – the Kaurik Chango Rift, LH – the Lesser Himalaya, GH – the Greater Himalaya, TH – the Tethyan Himalaya.

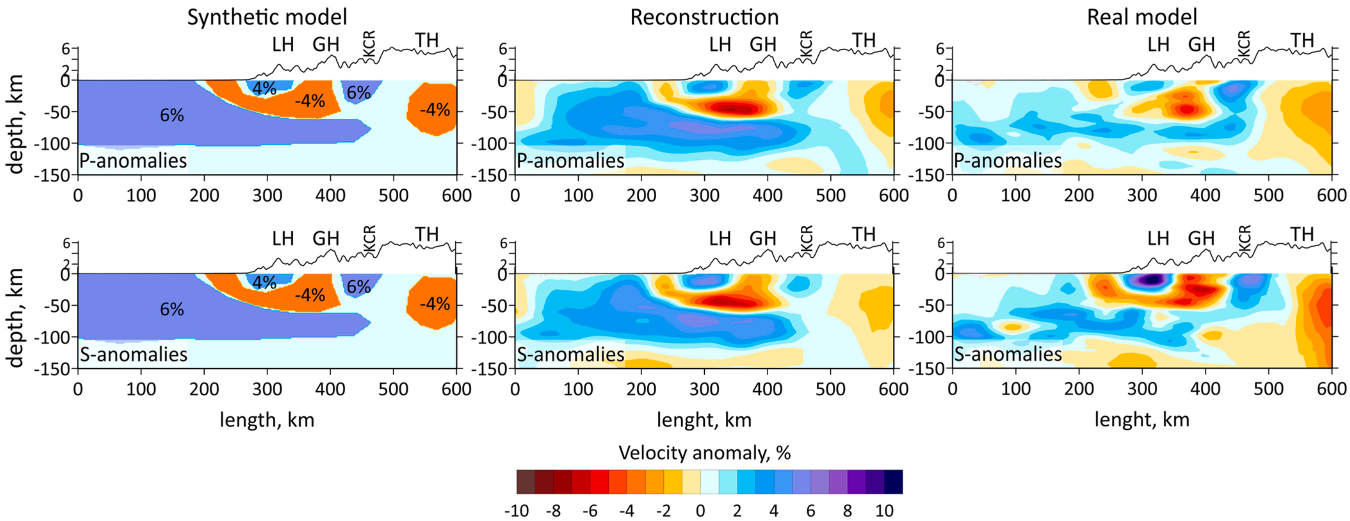

Fig. 9. Test with realistic anomalies along section b, the same as in Fig. 4. Column 1 represents synthetic model with value of anomaly amplitudes for P and S velocities; Column 2 shows reconstruction of real-shaped synthetic model for P and S velocity anomaly. Column 3 shows inversion result of real data along section b for P and S velocity anomaly, the same as result in Fig. 6 (III) b). Abbreviations: KCR – the Kaurik Chango Rift, LH – the Lesser Himalaya, GH – the Greater Himalaya, TH – the Tethyan Himalaya.

towards the south where underthrusting of the Indian Plate below the Indo Gangetic plains has initiated. This could be because the Delhi Haridwar Ridge would face more resistance while underthrusting below the Himalayas and a new front for underthrusting would accommodate the continuous push created by the northward-moving Indian Plate. We also evidence the overthrusting of the plate along this section.

As for the Kaurik Chango Rift, it is distinguished as a high-velocity anomaly, while rift zones in tomography are typically characterized by reduced-velocity anomalies. In the horizontal sections, the anomaly has an isometric shape with dimensions of ~100 × 100 km, and with reference to the vertical section b it is clearly traced up to a 50–60 km depth.

Besides the Kaurik Chango Rift, the southeastern part of the study area – between the STD and Karakoram Fault – has higher velocities. It is located in the Tethyan Himalaya formed as a result of squeezing, folding, and faulting of a large amount of sedimentary strata at the forefront of the Indian Plate ~50–25 Ma (Chatterjee et al., 2013). According to this, the Tethyan Himalaya should appear in the tomographic models as a low-velocity anomaly; however, one observes the opposite case. In the area, the Indotethys marginal sea was closing; as it appears from Chatterjee et al. (2013), it completely closed behind the ITSZ, leaving only the result of back-arc volcanism in the form of the Kohistan-Ladakh Arc. We assume that a small remnant of the Indotethys oceanic plate may have remained beneath the Tethyan Himalaya, sandwiched between the Himalayas and Tibet. It is worthy of note that remnants of oceanic plates in collision zones are quite common. Tomographic data point out that structures of this kind occur in Turkey (Medved et al., 2021a,b) and the Caucasus (Zabelina et al., 2016). We surmise that due to the change in the elastic properties of the Indian crust in the Delhi-Haridwar Ridge, this remnant did not undergo deformation but remained as a distinct dense block clearly identified as the high-velocity anomaly in our tomographic models.

5. Conclusions

We used the LOTOS algorithm for a local seismic tomography modeling to produce P- and S- velocity models for the northwestern Himalayas. The seismic data are derived from from the ISC and IMD catalogues. Synthetic simulation showed a fair resolution down to a 120 km depth.

In general, the obtained pattern of seismic heterogeneities corresponds to the geological setting of the studied region. On the one hand, the Himalayan orogenic belt stands out well as a low-velocity anomaly corresponding to the crust with the thickness of up to ~50 km - On the other hand, there is a trend of the high-velocity Indian Plate's submergence at depth $\geq$ 60 km beneath the Himalayas. This is confirmed by comparison with receiver function surveys in the area (Priestley et al., 2008). As it appears from the sections a, b and c, the Indian Plate underthrusts towards the north below the Himalayas (Fig. 6 (III)). Besides, it also bends down westwards as it gets closer to the Hindukush Region (section d, Fig. 6 (III)).

In the seismically active Delhi-Haridwar Ridge, there is a distinguishable heterogeneous crustal structure up to ~40 km related to the sediments of the Indo-Gangetic Plain along with a vast number of faults. Despite the expectations of many researchers about a possible subsidence of the Delhi-Haridwar Ridge under the Himalayas, for example (Arora et al., 1982; Lilley et al., 1981), our results have not confirmed it.

The Kaurik Chango Rift manifests itself as a high-velocity structure ~100 × 100 km in size and up to 50 km in thickness. We believe it to be a remnant of the oceanic crust left after the closure of the Indotethys Ocean.

The fragmentation of the Delhi-Haridwar Ridge softens the movement of the Indian Plate to the north. As a result, the Tethyan Himalaya crust at the Kaurik Chango Fault is consolidated and evident as a high-velocity anomaly.

A new front where underthrusting has begun is observed on the southern side of the Delhi-Haridwar Ridge. It is not the case along any other sections perpendicular to the trend of the Himalayas. This could be because the ridge resists underthrusting more than the sediments of the Indo-Gangetic Plains.

The Indian Plate underhtrusts the Himalayas towards the north. This observation is supported by numerous previous works. However, in this study we are the first to notice that the plate also bends downwards to the west as it approaches the Hindukush Mountains.

Finally, the thickness of the crust varies both across and along the trend of the Himalayas.

Declaration of Competing Interest

The authors declare that they have no known competing financial interests or personal relationships that could have appeared to influence the work reported in this paper.

Acknowledgement

The reported study was funded by the Russian Foundation for Basic Research, Russia, project number 19-35-60002 and as part of the Ministry of Science and Higher Education of the Russial Federation's state assignments for Sobolev Institute of Geology and Mineralogy, and Trofimuk Institute of petroleum Geology and Geophysics of the Siberian branch of the Russian Academy of Sciences.

References

Acton, C.E., Priestley, K., Gaur, V.K., Rai, S.S., 2010. Group velocity tomography of the Indo-Eurasian collision zone. J. Geophys. Res. Solid Earth 115(B12) 1-B12335 (16), B12335.

Armijo, R., Tapponnier, P., Mercier, J.L., Han, T.L., 1986. Quaternary extension in southern Tibet: field observations and tectonic implications. J. Geophys. Res. Solid Earth 91 (B14), 13803–13872.

Arora, B.R., Lilley, F.E.M., Sloane, M.N., Singh, B.P., Srivastava, B.J., Prasad, S.N., 1982. Geomagnetic induction and conductive structures in north-west India. Geophys. J. Int. 69 (2), 459–475. https://doi.org/10.1111/j.1365-246x.1982.tb04960.x.

Arora, B.R., Gahalaut, V.K., Kumar, N., 2012. Structural control on along-strike variation in the seismicity of the northwest. Himalaya. J. Asian Earth Sci. 57, 15–24. https://doi.org/10.1016/j.jseaes.2012.06.001.

Banerjee, P., Bürgmann, R., 2002. Convergence across the northwest Himalaya from GPS measurements. Geophys. Res. Lett. 29 (13), 30–31.

Bansal, B.K., Mohan, K., Verma, M., Sutar, A.K., 2021. A holistic seismotectonic model of Delhi region. Sci. Rep. 11 (13818) https://doi.org/10.1038/s41598-021-93291-9.

Bhatti, Z.I., Zhao, J., Khan, N.G., Shah, S.T.H., 2018. Structure of crust and upper mantle beneath NW Himalayas, Pamir and Hindukush by multi-scale double-difference seismic tomography. Phys. Earth Planet. Inter. 281, 92–102. https://doi.org/10.1016/j.pepi.2018.06.001.

Bijwaard, H., Spakman, W., Engdahl, E.R., 1998. Closing the gap between regional and global travel time tomography. J. Geophys. Res: Solid Earth 103 (B12), 30055–30078.

Buslov, M.M., De Grave, J., Bataleva, E.A., 2004. Cenozoic tectonics and geodynamic evolution of the Tien Shan mountain belt as response to India-Eurasia convergence. Himal. J. Sci. 2 (4), 106–107.

Chandra, U., 1978. Seismicity, earthquake mechanisms and tectonics along the Himalayan mountain range and vicinity. Phys. Earth Planet. Inter. 16, 109–131.

Chatterjee, S., Goswami, A., Scotese, C.R., 2013. The longest voyage: tectonic, magmatic, and paleoclimatic evolution of the Indian plate during its northward flight from Gondwana to Asia. Gondwana Res. 23 (1), 238–267. https://doi.org/10.1016/j.gr.2012.07.001.

Diehl, T., Singer, J., Hetényi, G., Grujic, D., Clinton, J., Giardini, D., Kissling, E., Gansser Working Group, 2017. Seismotectonics of Bhutan: Evidence for segmentation of the Eastern Himalayas and link to foreland deformation. Earth Planet. Sci. Lett. 471, 54–64. https://doi.org/10.1016/j.epsl.2017.04.038.

England, P., Molnar, P., 1997. The field of crustal velocity in Asia calculated from Quaternary rates of slip on faults. Geophys. J. Int. 130 (3), 551–582.

Gahalaut, V.K., Kundu, B., 2012. Possible influence of subducting ridges on the Himalayan arc and on the ruptures of great and major Himalayan earthquakes. Gondwana Res. 21 (4), 1080–1088. https://doi.org/10.1016/j.gr.2011.07.021.

Gansser, A., 1964. Geology of the Himalaya. Interscience, New York, N.Y, p. 298.

Guillot, S., Garzanti, E., Baratoux, D., Marquer, D., Mahéo, G., de Sigoyer, J., 2003. Reconstructing the total shortening history of the NW Himalaya. Geochem., Geophys., Geosys. 4 (7) https://doi.org/10.1029/2002GC000484.

Guo, Z., Gao, X., Wang, W., Yao, Z., 2012. Upper-and mid-crustal radial anisotropy beneath the central Himalaya and southern Tibet from seismic ambient noise tomography. Geophys. J. Int. 189 (2), 1169–1182. https://doi.org/10.1111/j.1365-246X.2012.05425.x.

Gupta, H., Gahalaut, V.K., 2014. Seismotectonics and large earthquake generation in the Himalayan region. Gondwana Res. 25 (1), 204–213. https://doi.org/10.1016/j.gr.2012.11.006.

Gupta, S., Mohanty, W.K., Prakash, R., Shukla, A.K., 2013. Crustal heterogeneity and seismotectonics of the national capital region, Delhi, India. Pure Appl. Geophys. 170 (4), 607–616. https://doi.org/10.1007/s00024-012-0572-7.

IMD (2021) ⟨https://seismo.gov.in/MIS/riseq/earthquake⟩.

International Seismological Centre (2021), On-line bulletin, https://doi.org/10.31905/D808B830.

Koulakov, I., 2009. LOTOS code for local earthquake tomographic inversion: Benchmarks for testing tomographic algorithms. Bull. Seismol. Soc. Am. 99, 194–214. https://doi.org/10.1785/0120080013.

Koulakov, I., Maksotova, G., Mukhopadhyay, S., Raoof, J., Kayal, J.R., Jakovlev, A., Vasilevsky, A., 2015. Variations of the crustal thickness in Nepal Himalayas based on tomographic inversion of regional earthquake data. Solid Earth 6 (1), 207–216. https://doi.org/10.5194/se-6-207-2015.

Koulakov, I., Gerya, T., Rastogi, B.K., Jakovlev, A., Medved, I., Kayal, J.R., El Khrepy, S., Al-Arifi, N., 2018. Growth of mountain belts in central Asia triggers a new collision zone in central India. Sci. Rep. 8 (1), 1–8. https://doi.org/10.1038/s41598-018-29105-2.

Kumar, A., Kumar, N., Mukhopadhyay, S., Baidya, P.R., 2017. Crustal and uppermost mantle structures in the frontal Himalaya and Indo-Gangetic basin using surface wave: tectonic implications. Quat. Int. 462, 34–49. https://doi.org/10.1016/j.quaint.2017.02.035.

Kumar, N., Aoudia, A., Guidarelli, M., Babu, V.G., Hazarika, D., Yadav, D.K., 2019. Delineation of lithosphere structure and characterization of the Moho geometry under the Himalaya-Karakoram-Tibet collision zone using surface wave tomography. Geol. Soc. Lond. Spec. Publ. 481 (1), 19–40. https://doi.org/10.1144/SP481-2017-172.

Kumar, P., Yuan, X., Kind, R., Kosarev, G., 2005. The lithosphere-asthenosphere boundary in the Tien Shan-Karakoram region from S receiver functions: Evidence for continental subduction. Geophys. Res. Lett. 32 (7) https://doi.org/10.1029/2004GL022291.

Larson, K.M., Bürgmann, R., Bilham, R., Freymueller, J.T., 1999. Kinematics of the India-Eurasia collision zone from GPS measurements. J. Geophys. Res.: Solid Earth 104 (B1), 1077–1093. https://doi.org/10.1029/1998JB900043.

Lilley, F.E.M., Singh, B.P., Arora, B.R., Srivastava, B.J., Prasad, S.N., Sloane, M.N., 1981. A magnetometer array study in northwest India. Phys. Earth Planet. Int. 25 (3), 232–240. https://doi.org/10.1016/0031-9201(81)90066-2.

Maurya, S., Montagner, J.P., Kumar, M.R., Stutzmann, E., Kiselev, S., Burgos, G., Purnachandra Rao, N., Srinagesh, D., 2016. Imaging the lithospheric structure beneath the Indian continent. J. Geophys. Res.: Solid Earth 121 (10), 7450–7468. https://doi.org/10.1002/2016JB012948.

Medved, I., Polat, G., Koulakov, I., 2021. Crustal structure of the Eastern Anatolia Region (Turkey) based on seismic tomography. Geosci 11 (2), 91. https://doi.org/10.3390/geosciences11020091.

Medved, I., Bataleva, E., Buslov, M., 2021. Studying the depth structure of the Kyrgyz tien shan by using the seismic tomography and magnetotelluric sounding methods. Geosci 11 (3), 122. https://doi.org/10.3390/geosciences11030122.

Miglani, R., Shahrukh, M., Israil, M., Gupta, P.K., Varshney, S.K., 2014. Geoelectric structure estimated from magnetotelluric data from the Uttarakhand Himalaya, India. J. Earth Syst. Sci. 123 (8), 1907–1918. https://doi.org/10.1007/s12040-014-0504-2.

Mitra, S., Priestley, K., Bhattacharyya, A.K., Gaur, V.K., 2005. Crustal structure and earthquake focal depths beneath northeastern India and southern Tibet. Geophys. J. Internat. 160, 227–248. https://doi.org/10.1111/j.1365-246X.2004.02470.x.

Mukhopadhyay, S., Sharma, J., 2010. Crustal scale detachment in the Himalayas: a reappraisal. Geoph. J. Int. 183, 850–860. https://doi.org/10.1111/j.1365-246X.2010.04755.x.

Ni, J., Barazangi, M., 1985. Active tectonics of the western Tethyan Himalaya above the underthrusting Indian Plate: the Upper Sutlej River Basin as a pull-apart structure. Tectonophys 112 (1–4), 277–295.

Oreshin, S.I., Vinnik, L.P., Kiselev, S.G., Rai, S.S., Prakasam, K.S., Treussov, A.V., 2011. Deep seismic structure of the Indian shield, western Himalaya, Ladakh and Tibet. Earth Planet. Sci. Lett. 307 (3–4), 415–429. https://doi.org/10.1016/j.epsl.2011.05.016.

Priestley, K., Jackson, J., McKenzie, D., 2008. Lithospheric structure and deep earthquakes beneath India, the Himalaya and southern Tibet. Geophys. J. Int. 172 (1), 345–362. https://doi.org/10.1111/j.1365-246X.2007.03636.x.

Priestley, K., Ho, T., Mitra, S., 2019. The crustal structure of the Himalaya: a synthesis. Geol. Soc. 483–516, 10.1144/SP483-2018-127.

Rai, S.S., Priestley, K., Gaur, V.K., Mitra, S., Singh, M.P., Searle, M., 2006. Configuration of the Indian Moho beneath the NW Himalaya and Ladakh. Geophys. Res. Lett. 33 (15) https://doi.org/10.1029/2006GL026076.

Raoof, J., Mukhopadhyay, S., Koulakov, I., Kayal, J.R., 2017. 3–D seismic tomography of the lithosphere and its geodynamic implications beneath the northeast India region. Tectonics 36 (5), 962–980. https://doi.org/10.1002/2016TC004375.

Ravi Kumar, M., Mishra, D.C., Singh, B., Raju, D.C.V., Singh, M., 2013. Geodynamics of NW India: subduction, lithospheric flexure, ridges and seismicity. J. Geol. Soc. India 81 (1), 61–78. https://doi.org/10.1007/s12594-013-0006-x.

Replumaz, A., Karason, H., Van Der Hilst, R.D., Besse, J., Tapponnier, P., 2004. 4-D evolution of SE Asia's mantle from geological reconstructions and seismic tomography. Earth Planet. Sci. Lett. 221 (1–4), 103–115. https://doi.org/10.1016/S0012-821X(04)00070-6.

Sandhu, M., Kumar, D., Teotia, S.S. Seismic Hazard evaluation to National Capital (Delhi) Region due to Delhi Haridwar Ridge, 16th Symposium on Earthquake Engineering, 20–22 December 2018.

Sheehan, A.F., de la Torre, T.L., Monsalve, G., Abers, G.A., Hacker, B.R., 2014. Physical state of Himalayan crust and uppermost mantle: Constraints from seismic attenuation and velocity tomography. J. Geophys. Res.: Solid Earth 119 (1), 567–580. https://doi.org/10.1002/2013JB010601.

Singh, A., Kumar, M.R., 2009. Seismic signatures of detached lithospheric fragments in the mantle beneath eastern Himalaya and southern Tibet. Earth. Planet. Sci. Lett. 288 (1–2), 279–290. https://doi.org/10.1016/j.epsl.2009.09.031.

Subedi, S., Hetényi, G., Vergne, J., Bollinger, L., Lyon-Caen, H., Farra, V., Gupta, R.M., 2018. Imaging the Moho and the Main Himalayan Thrust in Western Nepal with receiver functions. Geophys. Res. Lett. 45 (24), 13–222. https://doi.org/10.1029/2018GL080911.

Sychev, I.V., Koulakov, I., Sycheva, N.A., Koptev, A., Medved, I., El Khrepy, S., Al-Arifi, N., 2018. Collisional processes in the crust of the northern Tien Shan inferred from velocity and attenuation tomography studies. J. Geophys. Res.: Solid Earth 123 (2), 1752–1769. https://doi.org/10.1002/2017JB014826.

Thakur, V.C., 1992. Geology of Western Himalaya. Pergamon Press, Oxford, p. 363.

Thirunavukarasu, A., Kumar, A., Mitra, S., 2016. Lateral variation of seismic attenuation in Sikkim Himalaya. Geophys. Suppl. Mon. Not. R. Astron. Soc. 208 (1), 257–268. https://doi.org/10.1093/gji/ggw384.

Xu, Q., Liu, H., Yuan, X., Zhao, J., Pei, S., 2021. Eastward dipping style of the underthrusting Indian lithosphere beneath the Tethyan Himalaya illuminated by P and S receiver functions. J. Geophys. Res.: Solid Earth 126. https://doi.org/10.1029/2020JB021219.

Yin, A., 2006. Cenozoic tectonic evolution of the Himalayan orogen as constrained by along-strike variation of structural geometry, exhumation history, and foreland sedimentation. Earth-Sci. Rev. 76, 1–131. https://doi.org/10.1016/j.earscirev.2005.05.004.

Zabelina, I., Koulakov, I., Amanatashvili, I., Khrepy, S., Nassir, A., 2016. Seismic structure of the crust and uppermost mantle beneath Caucasus based on regional earthquake tomography. J. Asian Earth Sci. 119, 87–99. https://doi.org/10.1016/j.jseaes.2016.01.010.